U. Calif.

THE VAN ALLEN RADIATION BELT

T.A. Farley

The Van Allen Radiation Belt

Thomas A. Farley
Institute of Geophysics and Planetary Physics
University of California
Los Angeles

May 12, 1964

Preprint of an article prepared for the Encylopedia of Earth Sciences

A. The Van Allen Radiation Belt

The Van Allen Radiation belt is a doughnut-shaped region surrounding the earth at the geomagnetic equator, containing energetic protons and electrons trapped in the geomagnetic field. At the geomagnetic equator the region extends from a radial distance (measured from earth center) of about 1.1 earth radii to the radial distance at which the geomagnetic field is effectively terminated by streams of low energy particles from the sun. The position of the termination varies from about 10 earth radii at local noon to 20 earth radii, or more, at local midnight.

B. Charged Particle Motion in the Geomagnetic Field

In general, the motion of a charged particle in a magnetic dipole field can be obtained only by numerical integration. For particles whose cyclotron radius is small compared with the scale of the geomagnetic field, the guiding center approximation may be used to describe the motion. In this approximation the motion is separable into three components.

The first component is a circular motion perpendicular to the magnetic field lines with the local cyclotron period T_1 and cyclotron radius R_c. T_1 and R_c are given in gaussian units

by

$$T_1 = \frac{2\pi mc}{eB} \qquad R_c = \frac{v_\perp mc}{eB}$$

where m, e, and $v_\perp$ are, respectively, the particle mass, the particle charge, and the component of the particle velocity perpendicular to the field lines.

The second component is a motion along the field lines in the direction of increasing flux density to a point at which the particle is reflected, called the mirror point; and then a return to another mirror point, called the conjugate point, in the opposite hemisphere. This oscillatory motion has a period T_2 which is substantially longer than that of the first motion.

A schematic representation of these two motions is shown in Fig. 1. The pitch angle α of the particle is defined as the instantaneous value of the angle between the particle velocity vector and the direction of the magnetic field; the equatorial pitch angle α_o of a particle is illustrated in Fig. 1.

Since a static magnetic field can do no work on a charged particle, the total energy E of the particle is conserved. In the guiding center approximation, where the motions are separable,

this requires that the total flux through the circular orbit be constant. This is equivalent to the statement, called the first adiabatic invariant of the motion, that

$$\frac{\frac{1}{2}mv_{\perp}^2}{B} = \frac{\frac{1}{2}mv^2 \sin^2 \alpha}{B} = \text{constant} \quad \text{for non-relativistic particles}$$

or

$$\frac{p^2 \sin^2 \alpha}{B} = \text{constant} \quad \text{for relativistic particles}$$

where p is the particle momentum. From this invariant it follows that

$$\frac{\sin^2 \alpha_1}{B_1} = \frac{\sin^2 \alpha_2}{B_2}$$

where the subscripts refer to any pair of points along the particle trajectory. If we choose one of these points at the equator and the other at the mirror point, it follows that

$$\frac{B_m}{B_o} = \frac{1}{\sin^2 \alpha_o}$$

where B_m is the value of the field at the mirror point and B_o and α_o are equatorial values. Particles which have a value of α_o so

small that B_m will be at an altitude of 100 km or less will be rapidly removed by the earth's atmosphere and such particles must be absent under static conditions. The cone within which such pitch angles are found is called the loss cone.

A particle counter may be used at the geomagnetic equator to measure the unidirectional particle intensity at each pitch angle. The unidirectional intensity as a function of equatorial pitch angle is called the equatorial pitch angle distribution. This distribution, together with the first invariant, may be used to calculate both the unidirectional intensities and the omnidirectional intensity at all points on the same magnetic shell. Alternatively, a particle counter may be used to measure the omnidirectional intensity at every point along a field line. This description is equivalent to the equatorial pitch angle distribution which may be calculated from it.

A second adiabatic invariant of the motion is associated with the oscillatory motion between the mirror points. It may be stated as

$$J = \oint m v_{\parallel} \, ds = \text{constant}$$

where $v_{\parallel}$ is the component of the particle velocity directed along the field line. The integral is taken along the field line over

a complete oscillation of the particle between the mirror points.

The third motion of the particle is a slow drift in longitude with period T_3. Electrons drift from west to east and protons from east to west. The particle will slowly transfer itself from one flux tube to another until it finally drifts around the earth and returns to its original flux tube. In this process it generates what is known as a magnetic shell, surrounding the earth and open at both ends. A third invariant of the particle motion requires that the total number of lines of flux passing through this shell be constant. This statement is trivial for a static field, and is significant only for slowly varying time-dependent fields.

The guiding center approximation is thought to describe all the geomagnetically trapped radiation in the absence of strong electric fields or magnetic fields with time variations which are short compared with the characteristic periods T_1, T_2, and T_3. These three periods for typical trapped particles are given in Table I.

The particle motion is illustrated in Fig. 1 for a magnetic dipole. Since the geomagnetic field is only approximately a dipole, the particle motion is somewhat irregular even when described in geomagnetic rather than geographic coordinates.

TABLE I

Gyroradii and Periods of the Motions of Particles in the Guiding Center Approximation

L = 1.5

	R_c	T_1	T_2	T_3
Electrons				
50 kev	1.5×10^3 cm.	3.9×10^{-6} sec	.88 sec	6700 min
500 kev	4.7×10^3 cm.	4.2×10^{-6} sec	.30 sec	700 min
5 Mev	1.1×10^5 cm.	4.2×10^{-5} sec	.12 sec	12 min
Protons				
100 kev	2.8×10^5 cm.	7.1×10^{-3} sec	8.4 sec	340 min
1 Mev	8.8×10^5 cm.	7.1×10^{-3} sec	2.7 sec	34 min
10 Mev	2.8×10^6 cm.	7.2×10^{-3} sec	.85 sec	3.3 min
500 Mev	2.2×10^7 cm.	1.1×10^{-2} sec	.16 sec	.082 min

L = 4.0

	R_c	T_1	T_2	T_3
Electrons				
50 kev	2.8×10^4 cm.	7.4×10^{-5} sec	2.4 sec	2500 min
500 kev	9.0×10^4 cm.	8.1×10^{-5} sec	.79 sec	260 min
5 Mev	2.1×10^6 cm.	7.9×10^{-4} sec	.33 sec	4.6 min
Protons				
100 kev	5.3×10^6 cm.	1.3×10^{-1} sec	22.0 sec	130 min
1 Mev	1.7×10^7 cm.	1.3×10^{-1} sec	7.1 sec	12 min
10 Mev	5.3×10^7 cm.	1.4×10^{-1} sec	2.3 sec	1.3 min
500 Mev	-----	----	----	----

The gyroradii and periods have been computed according to the formulas of Hamlin, Karplus, Vik, and Watson, Jour. Geophys. Res., 66, 1-4, 1961. A dipole field is assumed. The periods are calculated for particles which mirror at a geomagnetic latitude of 30°. The gyroradius is given for the instant at which the particle crosses the geomagnetic equator.

A new coordinate system, defined by using the adiabatic invariants, has been devised to organize particle flux data. The three geographic coordinates r, λ, φ are transformed into two coordinates B and L. B is the scalar value of the field at r, λ, φ. L, given in units of earth radii, specifies the particular magnetic shell which passes through r, λ, φ. In a dipole field L would be the geocentric distance to the shell, measured in the geomagnetic equatorial plane. This L shell would be characterized by a certain minimum value of B, found on the geomagnetic equator of the shell. In a field which is only approximately a dipole, the same L shell has the same minimum value of B, but the trace of this minimum value around the shell is no longer a circle. The value of B at r, λ, φ is obtained from a spherical harmonic expansion of the geomagnetic field. L at r, λ, φ is obtained from a relatively lengthy machine computation utilizing the same expansion. A Fortran program for the computation has been widely distributed by McIlwain, who invented the coordinate system.

The value of the coordinate system lies in the fact that the particle intensity (in the absence of time variations and field distortions produced by outside influences)) is the same at all points having the same values of B and L. For a dipole field, this is simply equivalent to the statement that the particle intensity

does not depend on the magnetic longitude. This property of the coordinate system makes possible presentations of particle intensities as a function of only two coordinates B and L, rather than the three coordinates which are required to locate a point in space. Since presentations of data in the B, L representation do not lend themselves to simple geometric visualization, it is sometimes useful to define two dipole coordinates R, Λ according to the relations

$$B = \frac{M}{R^3}\left(4 - \frac{3R}{L}\right)^{1/2}, \quad R = L\cos^2\Lambda$$

where M is the magnetic dipole moment of the earth. This transformation makes possible a dipole-like presentation of the data in R, Λ space which permits easy visualization. R is the distance from the dipole source, and Λ is the magnetic latitude. Λ does not differ by more than a few degrees from the usual geomagnetic latitude λ_m, calculated from an earth-centered dipole model. A presentation of data in R, Λ space is shown in Fig. 2.

C. Early Experiments in the Radiation Belt

The term Van Allen Radiation Belt has historically been used to describe only those particles which have sufficient energy to be detected individually by a radiation counter suitable for

use in a space vehicle. This quite arbitrary threshold energy is about 40 kev for electrons, and about 100 kev for protons. The limitation is artificial, and the energy spectra of both types of particles extend downward to thermal energies, where relatively large number densities of protons and electrons are present everywhere in the exosphere. When thermal particles are included, the number densities of electrons and protons are equal and electrical neutrality is preserved, except perhaps in various transient phenomena.

Although the possibility of trapped radiation in the geomagnetic field has been known for many years, its presence was not established until 1958, when it was first detected by Van Allen and co-workers with instruments on the U.S. satellite Explorer I. Since that time numerous satellite and space probe measurements have been made by many scientific groups. The interpretation of early experiments was made difficult by the wide range of energies present and by the large time variations which occurred both in the energy spectra and the intensities of the trapped particles. Many early instruments could not distinguish electrons from protons, were often driven beyond their intended ranges, and responded to an unknown intensity of electron bremsstrahlung produced within the space vehicle.

A number of early experiments indicated the presence of two natural radiation belts, with a region of decreased intensity between. This apparent structure was probably, but not necessarily, instrumental in nature, caused by a continuous variation of the intensity and energy spectrum of both electrons and protons with distance from the earth. A more discriminating experiment has shown that at least one particle group does have two peaks (see Fig. 2). It is possible that other groups may have two (or more) peaks, and that the location of the peaks depends on the particular particle group and may also be time dependent. The division into two belts, sometimes called the inner and outer radiation zones, has persisted for reasons of history and convenience. The division does not necessarily indicate different origins for the particles in the two zones. In this description the boundary between the zones is taken to be at L = 2.

D. Energy Spectra and Distribution of Trapped Protons

Nuclear emulsion experiments have indicated that protons make up about 99 percent of the high-energy positively charged particle flux in the inner radiation zone. Deuterons and tritons make up the remainder. Particles of atomic number 2 or greater have not been detected. While the composition at low energies and in the outer zone has not been determined, most experimenters

have assumed that the positively-charged particles are protons in these regions as well.

Four measurements of the proton energy spectrum at different locations in the radiation belt are shown in Fig. 3. The two curves at L = 1.72 and L = 1.47 are representative of the inner zone. These two curves appear to indicate that a relatively strong source of low energy (5-30 Mev) protons contributes to the protons which are trapped on the magnetic shell at 1.72 earth radii, but not to the one at 1.47 earth radii. The peak intensity of high energy protons occurs between L = 1.4 and L = 1.5 where the omni-directional intensity of protons above 40 Mev at the geomagnetic equator is

$$J\ (> 40\ \text{Mev}) = 2 \times 10^{4}\ \text{proton cm}^{-2}\text{sec}^{-1}$$

The two curves at L = 2.8 and L = 5.0 are representative of the outer zone. The energy spectrum softens systematically with increasing radial distance in the outer zone, as indicated by the two curves. The reason for this softening depends on the source and loss mechanisms, which are not well understood. It is believed, however, that protons of tens and hundreds of Mev cannot be trapped in the outer zone because they would violate the adiabatic invariant conditions, and would escape rather quickly

from the geomagnetic field even if there were a source to place them there. The peak intensity of low energy protons in the outer zone occurs at about L = 3.5 where the unidirectional intensity is

$$j\ (100\ \text{kev} < E < 4.5\ \text{Mev}) = 6 \times 10^{7}\ \text{protons cm}^{-2}\text{sec}^{-1}\text{ster}^{-1}$$

In addition to these energetic trapped protons, an energy flux of 60 ergs $cm^{-2}sec^{-1}ster^{-1}$ due to protons or positive ions has been detected in the inner zone. This flux is due to protons in the energy range from 400 ev to 500 kev or to positive ions of similar magnetic rigidity.

Fig. 2 is given as an example of the spatial distribution of the intensities of trapped protons in an energy range in which two peaks appear. Electrons and protons in other energy ranges have intensity distributions which are somewhat similar, but may have greater or lesser extent in both invariant latitude and radial distance, and may have only one peak.

D. Energy Spectra and Distribution of Trapped Electrons

The omnidirectional intensity of electrons near the geomagnetic equator, having energies greater than 40 kev,

is approximately constant within an order of magnitude for L between 2 and 10. The omnidirectional intensity is

$$J\ (>40\ \text{kev}) \approx 10^{7}\ \text{cm}^{-2}\text{sec}^{-1}$$

Electrons having energies from 1-5 Mev have a peak intensity in the region near L = 4, and the electron spectrum becomes progressively softer at greater radial distances. The intensity of the high energy group can vary by a factor of 1000 or more in connection with disturbances of the geomagnetic field originating in a solar event, but the total intensity of electrons above 40 kev has time variations which are much smaller, perhaps only a factor of 10. An electron spectrum for the outer zone, constructed as a composite of a number of measurements, is shown in Fig. 4.

The natural electrons present in the inner zone were swamped by electrons artificially injected by a nuclear detonation before accurate energy spectra or intensities could be measured. The measurements which were made, however, did indicate that electrons having energies of one Mev or more were relatively much less abundant than in the outer zone, and were perhaps entirely absent.

F. Sinks and Sources of Trapped Particles

The intensity of electrons or protons at any given instant at some location in the geomagnetic field represents a balance struck between the mechanisms which are contributing trapped particles and those which are removing them. Evidence indicates that there is more than one significant source and more than one significant sink for each type of particle. If the sources and sinks are approximately constant or slowly varying in time, the intensities will not change rapidly. If either one is impulsive, the intensities will show correspondingly rapid increases or decreases.

The possibility has been considered that the trapped particles may have originated on the sun, and may have been injected directly into the radiation belt without local acceleration. Such injection is not possible in a static field because particles outside the geomagnetic field cannot enter the trapping region, just as particles inside may not escape. If time-dependent distortions occurred which permitted particles to enter, particles would also escape at the same time. Since deep-space probes have shown that energetic particle intensities in interplanetary space do not approach those in the trapping regions, even during geomagnetic storms, such a distortion would cause a net loss of

of particles rather than a gain. The search has therefore turned to more sophisticated and complicated mechanisms.

1. Particle Sinks

While sudden release of trapped particles into interplanetary space due to a gross temporary distortion of the geomagnetic field cannot be ruled out, it is more likely that most trapped particles are lost when their mirror points are lowered to the top of the atmosphere or their energies are lowered below the arbitrarily defined thresholds of the radiation belt. Several sinks which have been considered in some detail are as follows:

a. Collisions with electrons and ions (coulomb scattering).

This mechanism operates continuously to scatter both electrons and protons of all energies and, in some cases, to cause a significant energy loss of the energetic particle. Electrons are much more likely than protons to have significant angular deflection because of their lower masses. Some of the scattered particles will have lower mirror points than before, and some may therefore be lost in the atmosphere. This is equivalent to the statement that their new pitch angles are within the loss cone. This mechanism acts at all times, but may vary from time to time as the exospheric density changes.

b. Collisions with neutral atoms (ionization energy loss and charge exchange).

Ionization energy losses are more important than scattering effects for protons. Ionization energy losses of electrons are usually ignored, because they are small when compared with the scattering effects. Charge exchange, a process in which a proton picks up an electron from a thermal atom and becomes a fast neutral atom, is important only for protons below about 200 kev. The frequency of collisions with neutral atoms also depends on the exospheric density.

c. Nuclear collisions.

At proton energies above about 80 Mev, nuclear collisions constitute a more important loss mechanism than ionization energy loss, because of the decrease of the latter with increasing proton energy.

d. Scattering by hydromagnetic waves.

It has been proposed that hydromagnetic waves propagating inward from the geomagnetic field termination scatter high energy protons and set a maximum value for the proton energy which can be trapped at any L value. This existence of this effect has not yet been verified.

e. Scattering by very low frequency electromagnetic radiation (whistlers).

The suggestion has been made that VLF radiation propagating along a line of force may scatter electrons which are trapped along that line, and may even accelerate electrons if sychronism between the electron gyrofrequency and the Doppler-shifted wave frequency can be maintained. It is not known whether sufficient energy density exists at VLF frequencies in the radiation belt to provide either a sink or source of electrons.

f. Acceleration by electric fields.

Appropriate electric fields could serve as a sink or source or simultaneously as both. Such electric fields would influence both electrons and protons. The fields might be produced by charge separation or plasma instabilities in the exosphere, either as a local or large scale phenomenon. The energy for such mechanisms would presumably originate in the particle streams from the sun (solar wind), or in the rotational energy of the earth. Since the potential differences across distances the size of the earth are not likely to be more than 10^5 volts, such fields are likely to be of importance for low energy particles only. Production or loss of particles up to 50-100 kev of energy might be possible.

Specific and detailed mechanisms for producing these electric fields and maintaining them for the required time have not yet been described.

g. Electromagnetic radiation by an accelerated particle (synchrotron radiation).

The maximum energy of a trapped electron is limited by the emission of synchroton radiation. The limit is probably of the order of tens of Mev in the radiation belt. Synchrotron radiation was observed after the injection of electrons up to about 10 Mev by the nuclear detonation on July 9, 1962. Radio emissions from Jupiter have been tentatively identified as synchrotron emission from electrons trapped in a Jovian magnetic field.

h. Violation of the adiabatic invariants.

The treatment of particle motions by the guiding center approximation requires that the magnetic field have a very small change in a length of one gyroradius of any trapped particle. This requirement, instead of hydromagnetic wave scattering, may determine the maximum energy that a proton may have at any given L value. Protons having energies above the maximum would presumably find their way down into the atmosphere or out into interplanetary

space within a relatively short time. In addition, the guiding center approximation requires that any time variations in the field must be slow in comparison to the characteristic periods of the three motions (Table I). The third invariant in particular has a period which is long compared with some of the geomagnetic field variations which occur during a geomagnetic storm.. There is general agreement that violation of the third invariant will produce a diffusion of particles from a given L shell onto adjacent L shells. This diffusion will cause some trapped particles to be lost at the top of the atmosphere and others to be lost to interplanetary space.

It is also possible that violation of the third invariant serves as a source of trapped particles, permitting low energy solar wind particles to diffuse into the geomagnetic field from the outer boundary of the magnetosphere.

2. Sources for Trapped Protons

a. Inner Zone

Experiments performed since the discovery of the radiation belt have not shown impulsive additions to or losses from the protons above 30 Mev in the inner zone. The variations which have been

observed that are not due to experimental differences may have been caused by a redistribution of protons which were already present, or by a slow variation over the solar cycle. The observations are consistent with a weak but approximately constant source at energies above about 30 Mev. These protons may originate in a process called neutron albedo, in which very high energy (1 bev or more) galactic cosmic rays strike the earth's atmosphere and produce neutrons in various nuclear collisions. These neutrons then diffuse out of the atmosphere and escape from the earth. A certain fraction of them decay into protons and electrons in the radiation belt. This mechanism is generally thought to contribute at most only a small fraction of the trapped electrons, but it may produce most or all of the high energy trapped protons in the inner zone. This source may be supplemented at proton energies below about 200 Mev by solar neutrons emitted by the sun and decaying into protons in the inner zone, although solar neutrons have not yet been detected.

The loss mechanisms for these protons are probably ionization energy loss, nuclear collisions, and possibly slow diffusion due to violation of the third adiabatic invariant.

All of these source and loss mechanisms are slowly varying and would produce a trapped proton belt without short-term intensity fluctuations.

At energies below 30 Mev, the proton intensity depends rather strongly on L. The energy spectra given in Fig. 3 indicate that there were many more low energy protons on the shell at L = 1.72 than there were at L = 1.47 at the time the measurements were made. Either the source or the sink of these protons must vary strongly with L.

It has been suggested that solar cosmic ray neutron albedo would provide a suitable L-dependent source. Solar cosmic rays, which are emitted from the sun during solar flares, typically have energies of several hundred Mev. They are guided into the earth's polar caps by the earth's dipole field, and cannot theoretically penetrate into the trapping regions. In the atmosphere above the polar caps they produce neutrons in nuclear collisions in the same way that the higher energy galactic cosmic rays produce them all over the earth. The protons which are produced by the subsequent neutron decays can be trapped only on L shells for which L exceeds a certain minimum because of the geometrical effect of the source location at the polar caps, and the necessity that the decay proton have a velocity vector which results in a mirror point above the atmosphere. L shells located at low altitudes near the geomagnetic equator cannot be populated by this mechanism.

This source of low-energy protons would be impulsive since it depends on the irregular occurrence of a solar flare event.

Whether this source provides sufficient protons to account for the observations is not known. The loss mechanisms for the low-energy protons are probably the same as those for protons above 30 Mev, and strongly L-dependent mechanisms have not been described.

b. Outer Zone.

It has been proposed that the low-energy protons in the outer zone are supplied by an inward diffusion of solar wind protons incident upon the magnetosphere at about 10 earth radii. This diffusion is the result of violation of the third adiabatic invariant by sudden magnetic impulses and disturbances which occur several times daily. Conservation of the first and second adiabatic invariants (which are not violated because of their much shorter periods), requires that the energies of the protons increase as they diffuse inward. Solar wind protons having energies of 10 kev or so at the magnetospheric boundary would have energies of 10 Mev or more at L equal 3 or 4.

Since the diffusion times increase sharply with decreasing L, it is doubtful that this mechanism could supply protons at L values lower than 3 or 4. Loss mechanisms would prevent the very long residence times required to build up an appreciable intensity at lower L values.

Since the intensity of these protons has been observed to increase during a geomagnetic storm, it is tempting to identify them (and possibly lower-energy undetected protons) as the source of the 'ring current' which causes the main phase depression in the horizontal component of the earth-surface field. Such a depression typically follows a sudden commencement geomagnetic storm, and usually lasts for a few days. This may be the time required for the charge-exchange process to remove the excess protons which diffused inward at the start of the storm.

Sufficient experimental evidence is not at hand to verify inward diffusion as the source of these protons, nor to confirm that they are the source of the "ring current".

3. Sources for Trapped Electrons

a. Inner Zone

The energy spectrum and intensity of electrons in the inner zone was not established unambigiously before the nuclear detonation which took place in the inner zone on July 9, 1962. This detonation injected large numbers of fission product decay electrons into trapped orbits and temporarily made study of the natural electrons impossible. Measurements made before the detonation indicated that

electrons having energies of 1 Mev or more were few in number, or perhaps entirely absent. The possibility exists that the same neutron decays which produced the energetic protons may have produced the electrons in this region. If they were produced in this way, the energy spectrum should have contained very few electrons above the 780 kev end point of the neutron beta decay spectrum.

The Project Starfish nuclear detonation occurred on July 9,1962 at an altitude of 400 km above Johnston Island in the Pacific Ocean. Some months later, the measured omnidirectional electron intensities at L = 1.2 near the geomagnetic equator were

$$J(> 500 \text{ kev}) = 3 \times 10^{9} \text{ electrons cm}^{-2}\text{sec}^{-1}$$

and

$$J(> 5 \text{ Mev}) = 1 \times 10^{7} \text{ electrons cm}^{-2}\text{sec}^{-1}$$

The intensity of these electrons is decreasing quite slowly, and some of them will be present for years. At least six other detonations have taken place at high altitudes at L values less than 1.2 or more than 1.7. These injections produced observable effects for several weeks at most. Evidently electrons on shells for which L is less than 1.2 are removed rather quickly by atmospheric scattering,

while those for which L is greater than 1.7 are removed rather quickly by transient phenomena which are characteriatic of the outer zone. The injection of these electrons has tended to obscure the natural processes in the inner zone, but it has certainly established the fact that electron lifetimes in this region are long, and that a weak source would be adequate to populate it. If no catastrophic events occur to dump these electrons, it will not be possible to study the natural source of electrons in this region for a long time. Both the energies and the spatial distribution of these artificial electrons may be substantially modified by natural processes before they are ultimately lost.

b. Outer Zone

In order to understand the source and loss mechanisms for outer zone electrons, considerable attention has been given to the lifetime of outer zone electrons. A number of satellite experiments have shown that the intensity of electrons in the heart of the outer zone can remain virtually constant for days at a time. Other measurements, made on high-altitude balloons and low-altitude satellites have shown large fluxes of electrons pouring downward into the upper atmosphere.

These fluxes have been sufficiently large, particularly at geomagnetically active times, to empty out the portion of the radiation belt which is directly overhead in a time of the order of minutes. This phenomenon, which is called electron precipitation, is almost always present to some extent under lines of force which connect with the outer radiation zone. Since the intensity of trapped electrons is not sufficient to sustain this drain when it is most intense, the precipitated electrons probably are not trapped particles being lost from the outer zone, but are instead fresh particles being accelerated and driven down into the atmosphere by an unknown mechanism. Observations at about 1000 km altitude indicate that when precipitation occurs the intensity of trapped particles at this altitude increases and becomes approximately equal to the intensity of particles being precipitated. This has been interpreted as evidence that the same mechanism which precipitates electrons also supplies energetic electrons to the radiation belt. Verification of the operation of this mechanism to produce trapped electrons at high altitudes is lacking.

The average rate of energy loss of precipitated electrons in the atmosphere is of the order of 4×10^{17} ergs per second. This corresponds to something like 1% of the average total kinetic energy which is incident on the magnetosphere in the solar wind. If the

solar wind supplies the energy for precipitation, the coupling mechanism must be rather efficient. An alternative source of this energy may be the earth's axial rotation. Since the plasma trapped in the magnetosphere co-rotates with the earth, the diurnal plasma motions caused by the deformation of the magnetosphere by the solar wind may produce electric fields to drive the precipitation. If this is the case, a way must be found for the geomagnetic variations which occur during periods of solar activity to trigger the release of energy from the large reservoir of the earth's rotational energy, in order to account for the correlation between geomagnetic activity and electron precipitation. Details of such a mechanism have not been presented.

REFERENCES

Farley, T.A., The Growth of Our Knowledge of the Earth's Outer Radiation Belt, Revs. of Geophys., 1, 3-34, 1963.

Hess, W.N., Energetic Particles in the Inner Van Allen Belt, Space Sci. Revs., 1, 278-312, 1962-1963.

LeGalley, D.P., and A. Rosen, editors, Space Physics, John Wiley and Sons, New York, 1964.

McIlwain, C.E., Coordinates for Mapping the Distribution of Magnetically Trapped Particles, J. Geophys. Res., 66, 3681-3691, 1961.

Northrop, T.G., Adiabatic Charged-Particle Motion, Revs. of Geophys., 1, 283-304, 1963.

O'Brien, B.J., Review of Studies of Trapped Radiation with Satellite-Borne Apparatus, Space Sci. Revs., 1, 415-484, 1962-1963.

FIGURE CAPTIONS

1. Schematic representation of adiabatic charged particle motion. The particle spirals around a flux tube as it bounces back and forth between mirror points. It simultaneously drifts slowly in longitude around the earth. The particle equatorial pitch angle is α_o.

2. A representative charged particle intensity distribution in the idealized dipole coordinates R, Λ. This distribution, which applies to protons from 40 to 110 Mev, is from McIlwain, Science, 142, p.355, 1963.

3. Four examples of measured proton spectra in the radiation belt. L designates the magnetic shell and λ_m designates the magnetic latitude at which the measurements were made. The data at L = 5.0 and 2.8 are adapted from Davis and Williamson, Space Research III, edited by W. Priester, p. 372, John Wiley and Sons, 1963. The data at L = 1.72 and 1.47 are from Naugle and Kniffen, J. Geophys. Res., 68, p. 4073, 1963.

4. Typical electron spectrum near the position of peak intensity in the outer zone. This spectrum is a composite of many measurements.

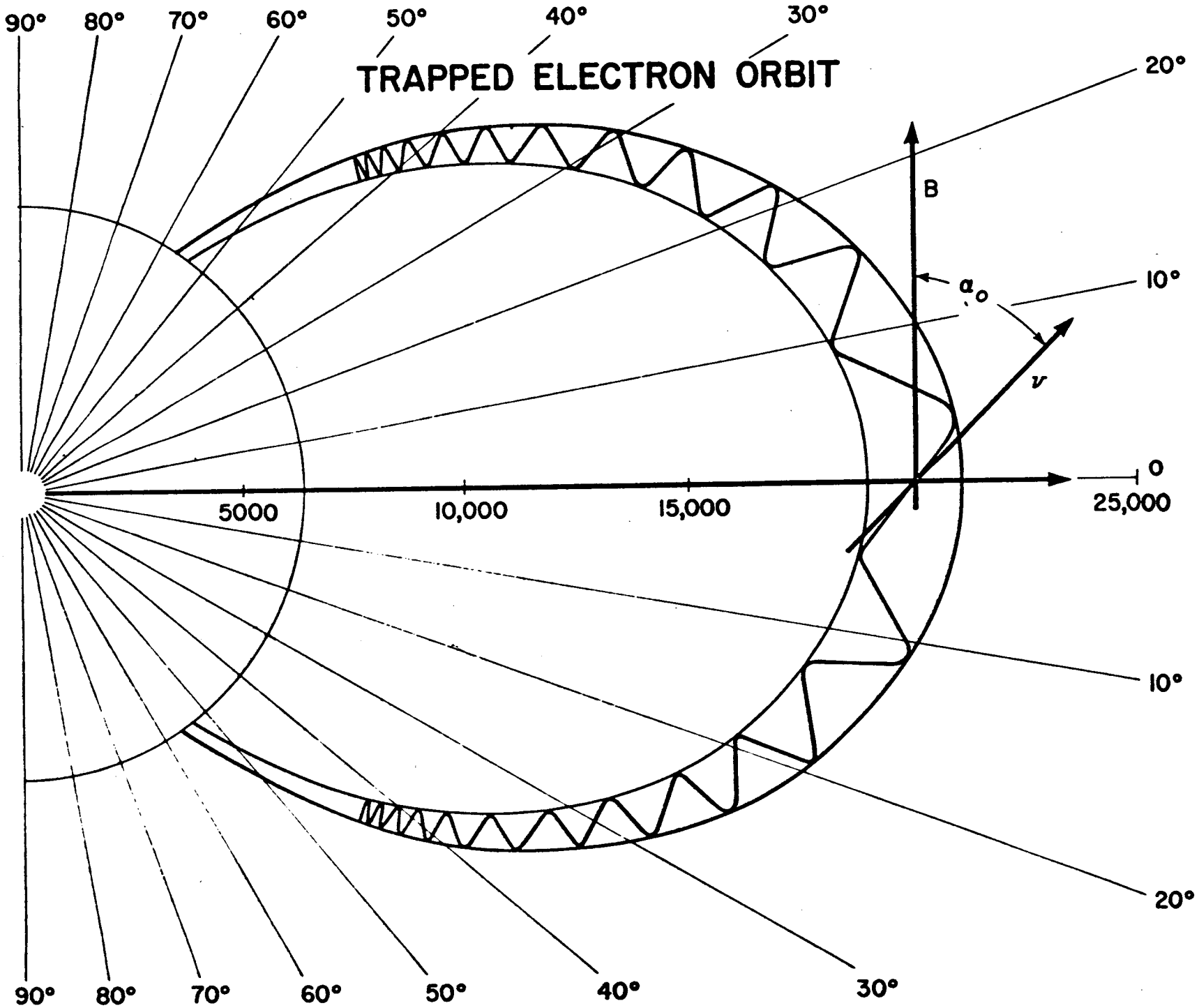
TRAPPED ELECTRON ORBIT
90°
80°
70°
60°
50°
40°
30°
20°
10°
0
10°
20°
B
α_o
v
5000
10,000
15,000
25,000

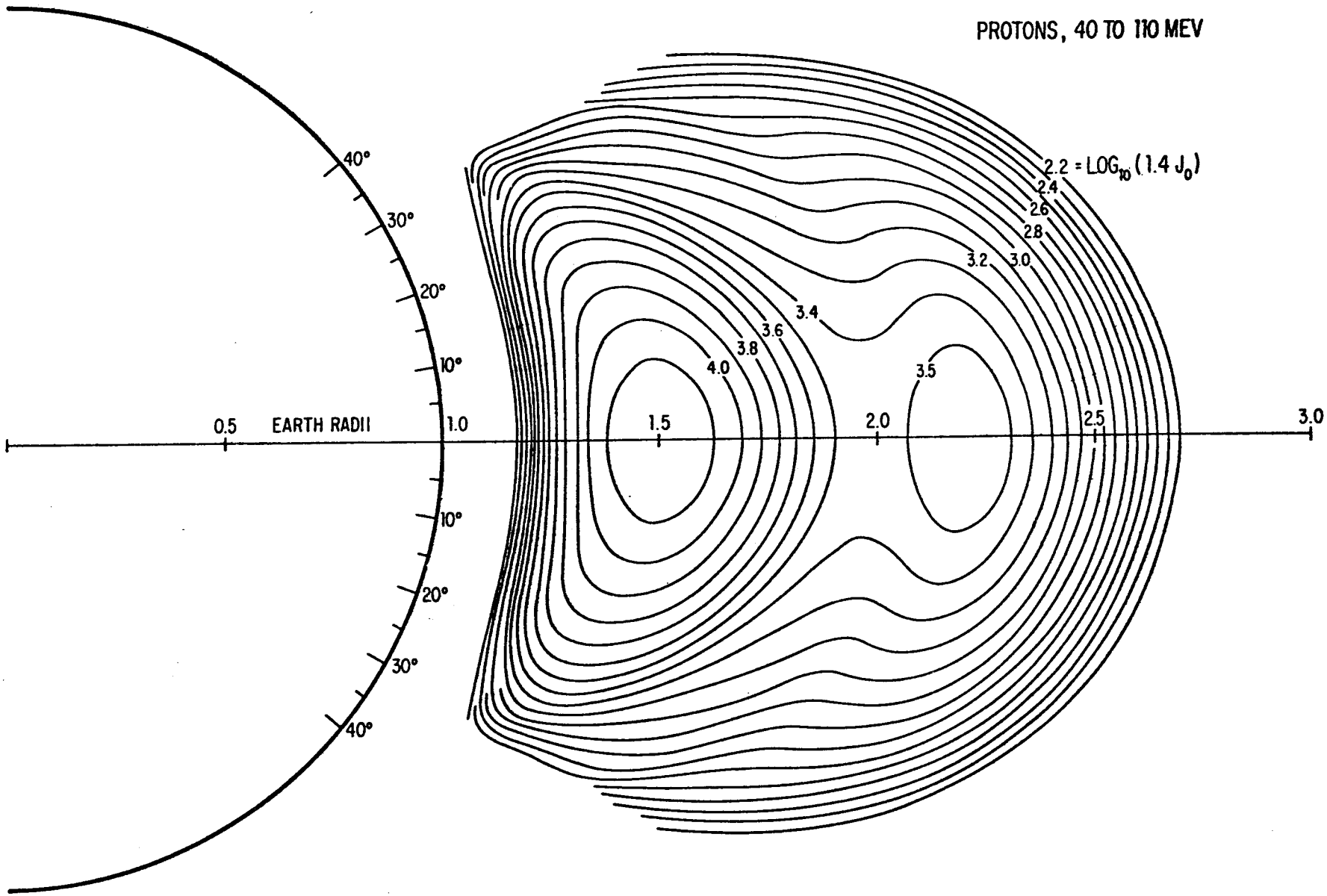
PROTONS, 40 TO 110 MEV
2.2 = LOG10 (1.4 J0)
2.4
2.6
2.8
3.0
3.2
3.4
3.6
3.8
4.0
3.5
40°
30°
20°
10°
10°
20°
30°
40°
0.5
EARTH RADII
1.0
1.5
2.0
2.5
3.0

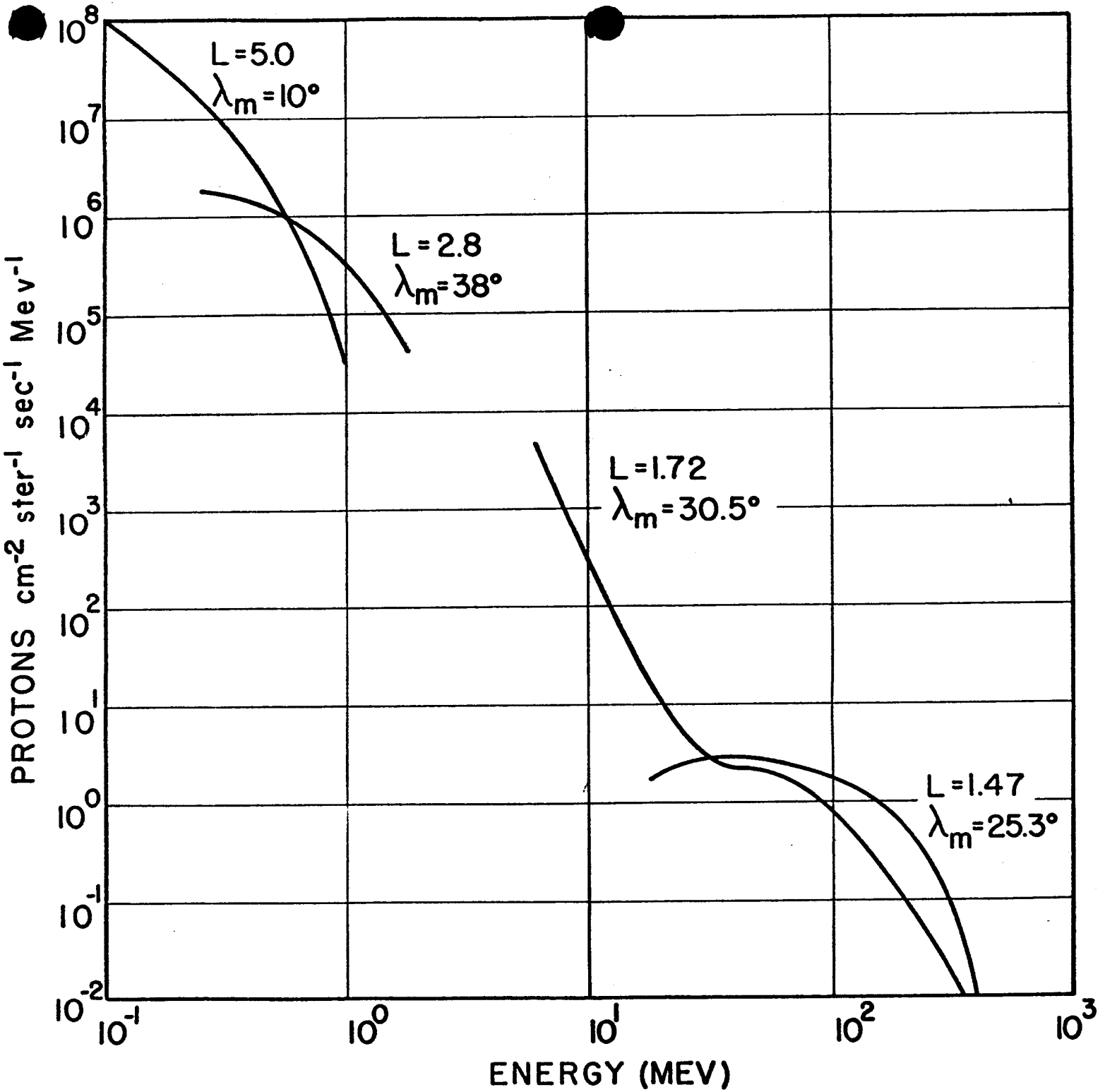
L=5.0
λ_m=10°
L=2.8
λ_m=38°
L=1.72
λ_m=30.5°
L=1.47
λ_m=25.3°
PROTONS cm^{-2} ster^{-1} sec^{-1} Mev^{-1}
ENERGY (MEV)
10^{8}
10^{7}
10^{6}
10^{5}
10^{4}
10^{3}
10^{2}
10^{1}
10^{0}
10^{-1}
10^{-2}
10^{-1}
10^{0}
10^{1}
10^{2}
10^{3}

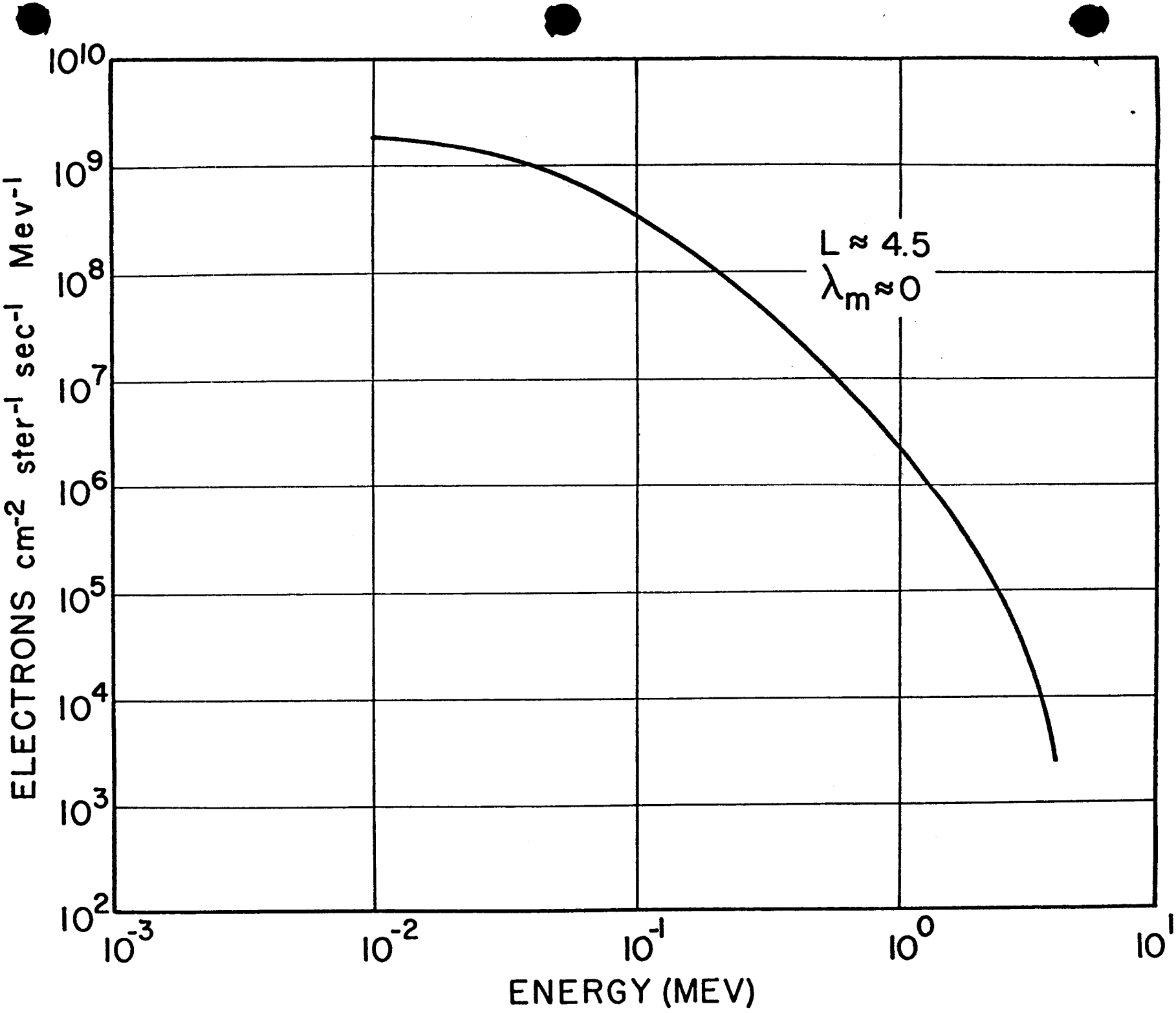
10^{10}
10^{9}
10^{8}
10^{7}
10^{6}
10^{5}
10^{4}
10^{3}
10^{2}
ELECTRONS cm^{-2} $ster^{-1}$ sec^{-1} Mev^{-1}
$L \approx 4.5$
$\lambda_m \approx 0$
10^{-3}
10^{-2}
10^{-1}
10^{0}
10^{1}
ENERGY (MEV)